Journal of Cellular Biochemistry 67:184–200 (1997)

v-*erbA* Oncogene Initiates Ultrastructural Changes Characteristic of Early and Intermediate Events of Meiotic Maturation in *Xenopus* Oocytes

Sylvia B. Nagl, Caroline F. Bunn, and Lizabeth A. Allison*

Department of Zoology, University of Canterbury, Christchurch, New Zealand

Abstract The growth-promoting properties of the retroviral v-*erbA* oncogene, a highly mutated version of the chicken thyroid hormone receptor (TR) α, have so far exclusively been linked to dominant repression of the antimitogenic roles of TR and retinoic acid receptors. Here we show that when expressed in *Xenopus* oocytes v-ErbA induced ultrastructural changes characteristic of early and intermediate events of meiotic maturation by activating gene transcription. v-ErbA–induced maturation events occurred without activation of the cAMP/maturation-promoting factor signal pathway and were arrested prior to meiotic spindle formation. The effects of v-ErbA were not mimicked by a dominant negative in vitro–generated mutant of human TR, suggesting that v-ErbA can contribute to cell cycle reentry by interference with regulatory pathways distinct from those involving TR. Interestingly, a portion of v-ErbA expressed in oocytes was present at the cytoplasmic fibrils of the nuclear pore complexes, suggesting that in addition to its intranuclear function v-ErbA may modulate nucleocytoplasmic transport. J. Cell. Biochem. 67:184–200, 1997.

Key words: maturation-promoting factor; meiosis; nuclear pore complex; nucleocytoplasmic transport; thyroid hormone receptor

The cooperative action of v-*erbA* and its retroviral partner v-*erbB*, both carried by the avian erythroblastosis virus, induces acute erythroblastosis and fibrosarcomas in young chicks. The v-*erbA* product, a highly mutated version of the chicken thyroid hormone receptor (TR) α, dominantly represses the actions of normal TR and retinoic acid receptors (RARs) [reviewed in Privalsky, 1992]. In addition, two mutations in the DNA binding domain, together with mutations in an N-terminal region, alter the range of DNA target sequences the v-*erbA* protein can bind to relative to TR [Chen et al., 1993; Smit-McBride and Privalsky, 1993; Subauste and Koenig, 1995]. While chicken embryo fibroblasts expressing only v-*erbA* do not display a fully transformed phenotype, they exhibit a greatly enhanced growth potential and a decreased requirement for growth factors [Gandrillon et al., 1987].

Contract grant sponsors: Cancer Society, Lottery Health Research, Health Research Council of New Zealand.

*Correspondence to: Lizabeth A. Allison, Department of Zoology, University of Canterbury, Private Bag 4800, Christchurch 8001, New Zealand.
E-mail: l.allison@zool.canterbury.ac.nz

Received 2 June 1997; accepted 18 June 1997

The growth-promoting properties of v-ErbA have so far been linked to dominant repression of the antimitogenic roles of TR and RAR. This mode of action is indicated by the fact that v-*erbA* is able to stimulate proliferation by overcoming growth inhibition by retinoic acid [Sharif and Privalsky, 1991]. In this context, v-*erbA* function is strongly correlated with its action as a dominant negative oncogene in abolishing AP-1 repression by RAR and TR [Desbois et al., 1991a,b; Zhang et al., 1991]. Furthermore, in the presence of v-*erbA*, erythrocytic progenitor cells are insensitive to the induction of apoptosis and self-renewal inhibition by retinoic acid or thyroid hormone [Gandrillon et al., 1994]. The question of whether the growth-promoting properties of v-ErbA can be exclusively attributed to dominant repression of TR and RAR or whether they also involve the activation of specific v-ErbA–responsive genes remains unanswered to date. Thus, we sought to determine whether it was possible to identify a direct role of v-ErbA in cell cycle induction at the level of gene transcription by employing meiotic maturation assays.

Meiotic maturation assays carried out in fully grown (stage VI) [Dumont, 1972] oocytes from

Xenopus laevis, the African clawed frog, have been used extensively for studies of oncogene involvement in the kinase signal cascades of the cell cycle [reviewed in Smith, 1989]. Fully grown oocytes are arrested at the G_2/M border and can be induced to enter M-phase by progesterone, insulin, and a range of introduced oncogenic protein kinases. Within minutes of progesterone exposure, a decrease in levels of cAMP occurs, mediated by inhibition of adenylate cyclase, which in turn downregulates protein kinase A and protein kinase C activities [Smith, 1989]. The induction of *Xenopus* oocyte maturation by progesterone does not require gene transcription but is absolutely dependent on polyadenylation and translation of stored mRNA coding for the serine-threonine kinase Mos [Baltus et al., 1973; Sagata et al., 1988; Yew et al., 1992; Sheets et al., 1995]. A network of phosphorylation cascades [Kosako et al., 1994a,b; reviewed in Mordret, 1993] culminate in the activation of maturation-promoting factor (MPF) and mitogen-activated protein kinase (MAPK). MPF contains the *Xenopus* homolog of the universal M-phase inducer $p34^{cdc2}$, a serine-threonine kinase with histone H1 phosphorylating activity, which is complexed with B-type cyclins [Maller, 1990]. MPF and MAPK trigger the events of maturation, including nuclear breakdown, chromosome condensation, and meiotic spindle formation [Smith, 1989; Bement and Capco, 1990].

In fully grown (stage VI) oocytes, the chromosomal loops associated with high transcriptional activity during earlier stages of oogenesis have retracted considerably, and the chromatin is quite condensed [Hausen and Riebesell, 1991]. Thus, although microinjected gene templates are transcribed efficiently in stage VI oocytes [Nagl et al., 1995], it was an open question whether *Xenopus* homologs of potential target genes would be accessible to v-ErbA and the general transcription machinery in stage VI oocytes.

In the present study, we show that v-ErbA initiates ultrastructural changes characteristic of early and intermediate meiotic events, but meiosis was arrested prior to spindle formation. The initiation of this subset of maturation events by v-ErbA required de novo gene expression and did not involve activation of the cAMP/MPF signal pathway. Events induced by v-ErbA were not mimicked by a dominant negative in vitro–generated mutant of TR, suggesting that the ultrastructural changes were not mediated by dominant repression of endogenous TR. Our study suggests that v-ErbA, acting as a transcriptional activator, can contribute to cell cycle reentry by interference with regulatory pathways distinct from those involving TR.

MATERIALS AND METHODS

Plasmids

RS-v-*erbA* was a gift from R. Evans (Salk Institute for Biological Studies, La Jolla, CA). The expression vector contains the *gag*-v- *erbA* oncogene cDNA under the transcriptional control of the Rous sarcoma virus (RSV) long terminal repeat (LTR) [Damm et al., 1989; Thompson and Evans, 1989]. The RSh-TRβ C122>A expression plasmid was a gift of P. Romaniuk (University of Victoria, Victoria, BC, Canada). It contains an in vitro–generated mutant human TRβ gene (alanine instead of cysteine at position 122) under control of the RSV LTR [Nelson et al., 1993]. pRSV-*lacZ* was obtained from M. Harkey (University of Washington, Seattle, WA) and contains the *E. coli* β-galactosidase gene under control of the RSV LTR [Gorman et al., 1983]. The pKCR2-cea plasmid was a gift of B. Vennström (Karolinska Institute, Stockholm, Sweden) and contains the chicken *c-erbA* cDNA expressed from the SV-40 promoter [Sap et al., 1989]. The pGEM-4Z vector was a gift of M. Privalsky (University of California, Davis, CA), and contains the *gag*-v-*erbA* cDNA under control of the SP6 RNA polymerase promoter.

Oocyte Microinjections

A lobe of ovary was surgically removed from an adult female *Xenopus laevis* and processed as described [Allison et al., 1991, 1993]. Microinjections were performed according to published methods with modifications [Nagl et al., 1995]. Defolliculated stage VI oocytes [Dumont, 1972] were microinjected with 5 ng expression vector in a fixed volume of 20 nl TE (10 mM Tris-HCl, pH 8.0, 1 mM EDTA) into the nucleus by the "blind" injection method with the needle inserted in the center of the animal pole. Alternatively, v-*erbA* protein was synthesized from the pGEM-4Z template by in vitro coupled transcription/translation in rabbit reticulocyte lysate (Promega, Madison, WI), according to the manufacturer's specifications, using SP6 RNA polymerase. Fifty nanoliters v-*erbA* solution (approximately 100 pg v-ErbA in rabbit reticulo-

cyte lysate) was microinjected into the oocyte cytoplasm.

Incubation Treatments and Assessment of Germinal Vesicle Migration and Germinal Vesicle Breakdown

Oocytes were incubated in O-R2 medium [Allison et al., 1991] only or in O-R2 containing (1) 10 μg/ml progesterone (Sigma Chemical Co., St Louis, MO), (2) 20 μM forskolin (Sigma) and 2 mM isobutylmethylxanthine (IBMX) (Sigma); (3) 30 μg/ml actinomycin D (actinomycin C_1) (Boehringer Mannheim NZ Ltd., Auckland, New Zealand), or (4) 200 μg/ml cycloheximide (BDH Chemicals NZ Ltd., Palmerston North, New Zealand). Twenty-four hours after nuclear microinjection with 5 ng RS-v-*erbA* or pRSV-*lacZ* or cytoplasmic injection of 50 nl of in vitro–synthesized v-*erbA* protein, oocytes were scored for germinal vesicle migration (GVM) under a stereomicroscope, as indicated by pigment rearrangement at the apical pole that produces a whitish circular spot delineated by a dark ring of pigment [Smith, 1989; Bement and Capco, 1990; Brachet et al., 1970]. Oocytes were assessed for germinal vesicle breakdown (GVBD) by manual dissection after fixation in ice-cold 1% trichloroacetic acid (TCA) for 5 min. Oocytes were scored positive for GVBD when the nucleus could not be dissected intact due to nuclear instability.

Differential Interference Contrast Microscopy

Oocytes incubated in progesterone or microinjected with 5 ng RS-v-*erbA*, RSh-TRβ C122 > A, or pRSV-*lacZ* were fixed and embedded essentially as described by Hausen and Riebesell [1991]. In brief, oocytes were fixed in Romeis fixative (25 ml saturated mercuric chloride, 20 ml 5% TCA, 15 ml 37% formaldehyde) for 3 h. Subsequently, oocytes were dehydrated in an ethanol series of 50% (15 min), 70% (30 min), 80% (15 min), 90% (15 min), 95% (15 min), and 100% (3 × 10 min), infiltrated in 50% glycol methacrylate infiltration solution (Polaron, Auckland, New Zealand) in ethanol for 1 h, and then left in 100% infiltration solution overnight. Oocytes were embedded in glycol methacrylate (Polaron) in gelatine capsules under nitrogen at 37°C for 5 h. Five micron sections were obtained with Ralph glass knives. In order to remove mercury precipitates, we treated the dry sections with an alcoholic iodine potassium iodide solution (2% iodine, 3% potassium iodide in 90% ethanol) for 2 min, washed them in 0.25% sodium thiosulfate for 15 min, and thoroughly rinsed them in distilled water. The sections were stained utilizing an azofuchsin/aniline blue/orange G triple-staining method [Hausen and Riebesell, 1991]. Three independent batches of oocytes were used, and three to four oocytes per treatment per batch were analyzed using differential interference contrast microscopy. Oocyte sections were photographed using Agfa optima color film with a blue filter.

Electron Microscopy for Ultrastructural Analysis

In ultrastructural studies of *Xenopus* oocytes, long fixation times and special fixation procedures are necessary. Unless indicated otherwise, all procedures were carried out at 4°C. Oocytes were fixed in 2.5% glutaraldehyde and 0.05% low molecular weight tannic acid in O-R2 overnight, washed in O-R2 three times for 30 min, and subsequently transferred to 2% OsO_4 (in ddH_2O) for 3 h with one change. Oocytes were then washed in O-R2 for 30 min and dehydrated in a graded ethanol series of 30% (30 min), 50% (30 min), 70% (overnight), 80% (20 min), 90% (20 min), 95% (15 min), and 100% (2 × 15 min). After the 70% ethanol step, all further procedures were carried out at room temperature. Oocytes were incubated in 100% acetone twice for 20 min and then gradually embedded in Spurr's resin in acetone: 30% resin (1 h), 50% resin (3 h), 70% resin (overnight), 90% resin (8 h), and 100% resin (overnight). Oocytes were transferred into 100% resin in molds and cured at 70°C for 24 h. Ultrathin sections (50 nm) were stained with 5% uranyl acetate in 50% ethanol for 20 min, washed in ddH_2O, stained with lead citrate for 20 min, and put through a final washing step in ddH_2O. Three independent batches of oocytes were used, and three to four oocytes per treatment per batch were analyzed.

Histone H1 Kinase Assay

Adult female *Xenopus laevis* were injected with 0.5 ml gonadotropin (from pregnant mares' serum (Sigma); 200 U/ml in sterile ddH_2O) subcutaneously into the dorsal lymph sac to improve the synchrony of response to progesterone in oocytes. After 4 days, a lobe of ovary was surgically removed from the animal and processed as described above. Defolliculated stage VI oocytes were microinjected into the nucleus with 5 ng RS-v-*erbA* or pRSV-*lacZ* or incubated in 10 μg/ml progesterone. At specified times, oocyte extracts were prepared by homogenizing

groups of ten oocytes in 20 µl extraction buffer (20 mM Tris, pH 7.5, 80 mM β-glycerophosphate, 20 mM EGTA, 15 mM $MgCl_2$, 25 µg/ml aprotinin, 25 µg/ml leupeptin, 1 mM benzamidine, 0.5 mM phenylmethylsulfonyl fluoride (PMSF), 5 mM Pefabloc (Boehringer Mannheim), and 1 mM DTT). The homogenate was centrifuged at 10,000*g* for 10 min at 4°C to pellet yolk and pigment. Ten microliters of the supernatant were mixed and incubated for 20 min at 25°C with 10 µl kinase buffer (30 mM Tris, pH 7.5, 30 mM $MgCl_2$, 1 mCi/ml γ[^{32}P] ATP (Amersham Life Sciences, Auckland, New Zealand), 3 mg/ml histone H1 [Sigma]) [Kosako et al., 1994b]. The reaction was stopped by the addition of an equal volume of 2× SDS sample buffer (4% SDS, 20% glycerol, 120 mM Tris, pH 6.8, 0.01% bromophenol blue) and boiling for 5 min. Samples were resolved by 12% SDS-PAGE followed by autoradiography.

Immunoprecipitation of Oocyte Fractions With an Anti-v-erbA Antibody

Oocytes were microinjected with 5 ng RS-v-*erbA* or pKCR2-cea into the nucleus and incubated in a sterile microtitre plate (five oocytes/well) in 30 µl of O-R2 with 1 mCi/ml L-[^{35}S] methionine (1,000 Ci/mmol) (Amersham) at 18°C for 24 h. Nuclear fractions of 10 or 20 pooled v-*erbA*–injected oocytes were prepared manually, after fixation in 1% ice-cold TCA for 5 min [Allison et al., 1993]. Net-2 (50 mM Tris, pH 7.4, 150 mM NaCl, 0.05% Nonidet P-40) samples were homogenized in 0.5 ml NET-2 [Allison et al., 1993] containing 0.1 mM PMSF. For preparation of nuclear membrane fractions, nuclei were manually isolated in nuclear isolation medium (NIM) (83 mM KCl, 17 mM NaCl, 10 mM Tris, pH 7.2, 5 mM Pefabloc) [Krohne and Franke, 1983] in a small siliconized petri dish using watchmaker's forceps. Nuclei were freed from adhering yolk by aspirating them into a pipette with an inner bore diameter of 0.7–0.8 mm and then washed once in fresh NIM and transferred into nuclear envelope isolation medium (NEM) (83 mM KCl, 17 mM NaCl, 10 mM $MgCl_2$, 10 mM Tris, pH 7.2, 5 mM Pefabloc). Within 30–60 s, the nuclear content forms an opaque and compact aggregate from which the nuclear membrane (envelope) detaches. The nuclear membranes were isolated by aspirating nuclei into a pipette with an inner bore diameter of 0.3–0.4 mm, cleaned in fresh NEM by repeated aspiration into a small pipette, and transferred into a microfuge tube. Ten or 20 nuclear envelopes were pooled per sample and collected by centrifugation for 4 min at 8,000*g* and resuspended by gentle aspiration in 0.5 ml NET-2 containing 5 mM Pefabloc.

For total soluble protein electrophoretic separations, 20 µl 2× SDS sample buffer and 1 mM dithiothreitol (DTT) were added to 20 µl cleared homogenate from nuclear and nuclear membrane fractions, which were then resolved by 12% SDS–polyacrylamide gel electrophoresis and stained with Bio-Rad Silver Stain (Bio-Rad Laboratories Pty Ltd., Auckland, New Zealand).

For immunoprecipitation assays, 30 µl of monoclonal antibody LAO38 against v-*erbA* residues 58–75 (Quality Biotech, Camden, NJ) were bound to 20 µl preswollen protein G–Sepharose beads (Gamma Bind Plus Sepharose, Pharmacia LKB Biotechnology, Auckland, New Zealand) in 0.45 ml NET-2 for 2 h at room temperature with end-over-end rotation. After incubation, the resin was pelleted for 5 s in a microfuge and resuspended in 1 ml of NET-2, and the wash was repeated three times. Pooled nuclei or nuclear membrane samples in NET-2 were added to each washed protein G–Sepharose-antibody pellet and incubated at 4°C for 1 h with end-over-end rotation. After incubation, the resin with bound antigen was pelleted and washed four times with NET-2. Twenty microliters of 2× SDS sample buffer was added to each pellet, the samples were heat-denatured to release the antigen, and the resin was pelleted for 5 s in a microfuge. The supernatant (with 1 mM DTT added) was resolved by 12% SDS-PAGE followed by fluorography.

Immunolabeling of Isolated Nuclear Membranes

Oocytes were microinjected with 5 ng RS-v-*erbA* into the nucleus and incubated in O-R2 for 12–14 h. Nuclear membranes of 20 oocytes per sample were manually isolated as described above and fixed in 2% formaldehyde, freshly made from paraformaldehyde in phosphate buffered saline (PBS) (137 mM NaCl, 1.3 mM Na_2HPO_4, 2.5 mM NH_2PO_4, pH 7.2), for 10 min at 4°C. Immunolabeling with colloidal gold, employing a biotin-streptavidin bridging technique, was carried out following published procedures [Cordes et al., 1993] with modifications and according to the manufacturer's specifications (Amersham). Membranes were collected by centrifugation at 8,000*g* for 4 min and washed three times in PBS, pH 7.2, containing

50 mM NH_4Cl. Membrane samples were then resuspended in 24 µl PBS, pH 7.2, with 6 µl anti-v-*erbA* antibody LA038, and incubated for 2 h at room temp. Subsequently, membranes were centrifuged at 8,000*g* for 4 min, washed three times in PBS, resuspended in 99 µl PBS, pH 7.2, containing 1 µl biotinylated goat anti-mouse Ig antibody (Amersham), and then incubated for 2 h at room temperature. The samples were then washed with PBS, pH 7.2, as described above. Next, membranes were incubated in 38 µl PBS, pH 7.2, with 2 µl AuroProbe EM streptavidin 10 nm (Amersham) for 2 h at room temperature and washed in PBS as before. Membranes were fixed in 2.5% glutaraldehyde in PBS, pH 7.2, for 30 min at 4°C, washed three times in PBS, and treated with 2% aqueous OsO_4 for 30 min at 4°C, followed by several

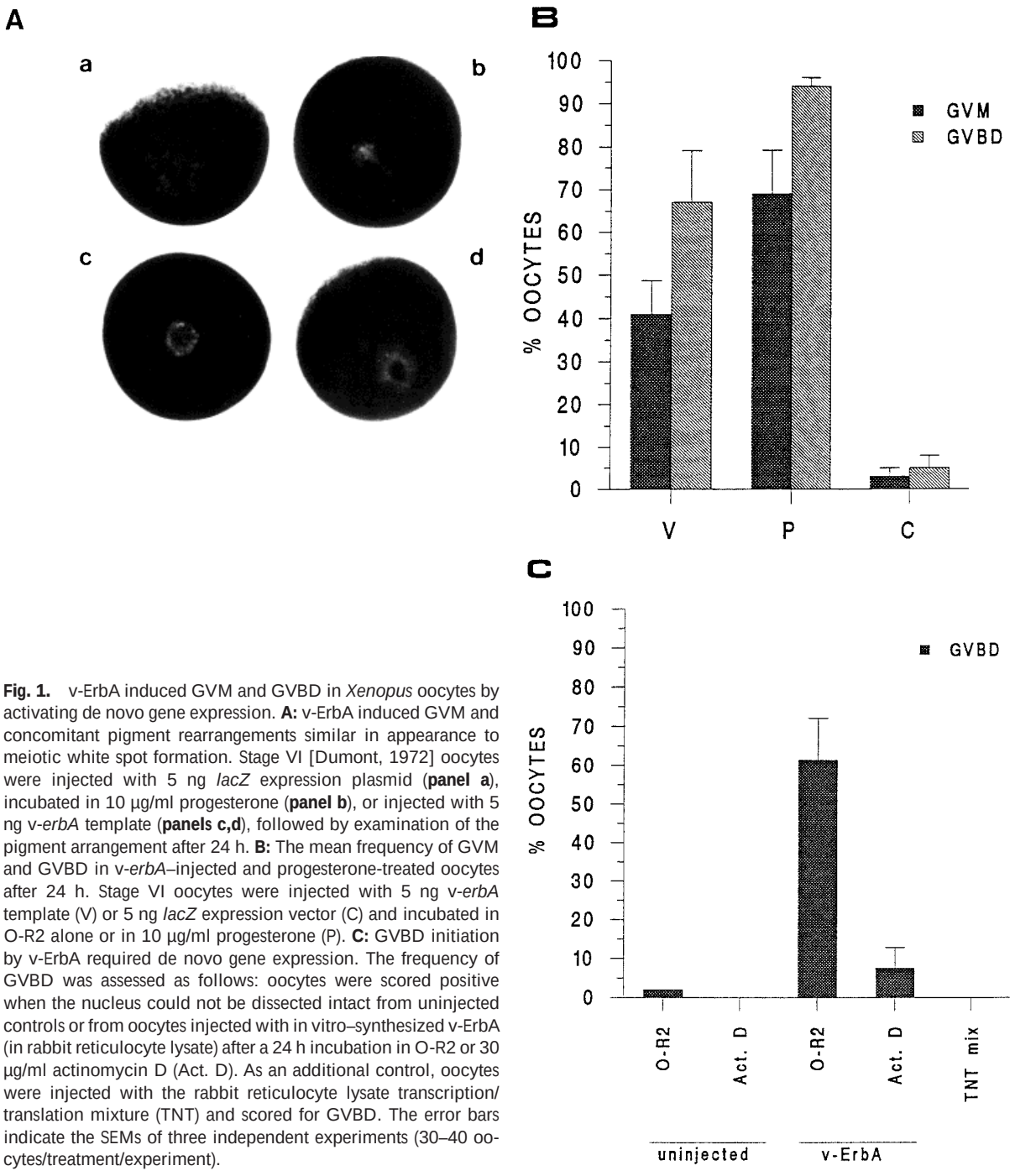

Fig. 1. v-ErbA induced GVM and GVBD in *Xenopus* oocytes by activating de novo gene expression. **A:** v-ErbA induced GVM and concomitant pigment rearrangements similar in appearance to meiotic white spot formation. Stage VI [Dumont, 1972] oocytes were injected with 5 ng *lacZ* expression plasmid (**panel a**), incubated in 10 µg/ml progesterone (**panel b**), or injected with 5 ng v-*erbA* template (**panels c,d**), followed by examination of the pigment arrangement after 24 h. **B:** The mean frequency of GVM and GVBD in v-*erbA*–injected and progesterone-treated oocytes after 24 h. Stage VI oocytes were injected with 5 ng v-*erbA* template (V) or 5 ng *lacZ* expression vector (C) and incubated in O-R2 alone or in 10 µg/ml progesterone (P). **C:** GVBD initiation by v-ErbA required de novo gene expression. The frequency of GVBD was assessed as follows: oocytes were scored positive when the nucleus could not be dissected intact from uninjected controls or from oocytes injected with in vitro–synthesized v-ErbA (in rabbit reticulocyte lysate) after a 24 h incubation in O-R2 or 30 µg/ml actinomycin D (Act. D). As an additional control, oocytes were injected with the rabbit reticulocyte lysate transcription/translation mixture (TNT) and scored for GVBD. The error bars indicate the SEMs of three independent experiments (30–40 oocytes/treatment/experiment).

washes in ddH_2O. Membrane samples were dehydrated in a graded ethanol series, incubated in 100% acetone twice for 20 min, and embedded in Spurr's resin in acetone: 50% resin (1 h), 90% resin (overnight), and 100% resin (1 h). Membranes were then immersed in fresh resin and cured at 70°C for 14 h. Ultrathin sections (50 nm) were stained with 2% uranyl acetate in 50% ethanol for 10 min, washed in ddH_2O, stained with lead citrate for 5 min, and washed in ddH_2O.

RESULTS

v-ErbA Induced GVM and GVBD in *Xenopus* Oocytes by Activating De Novo Gene Expression

During meiosis, pigment granules in the animal hemisphere cortex of *Xenopus* oocytes are rearranged, producing a whitish circular spot [reviewed in Smith, 1989]. Pigment displacement commences during early maturation and is thought to be initiated by structural changes in the oocyte cortex immediately upon meiotic induction [Bement and Capco, 1990]. The progressive migration of the nucleus (germinal vesicle migration), from near the center of the oocyte toward the animal pole, contributes to the rearrangement of pigment granules. Upon germinal vesicle breakdown and completion of maturation, a clearly delineated white spot represents the area where the meiotic spindle has formed [reviewed in Smith, 1989; Bement and Capco, 1990; Brachet et al., 1970].

We first tested the ability of v-ErbA to initiate maturation in *Xenopus* oocytes by comparing the rate of nuclear migration and breakdown in progesterone-treated and v-*erbA*–injected oo-

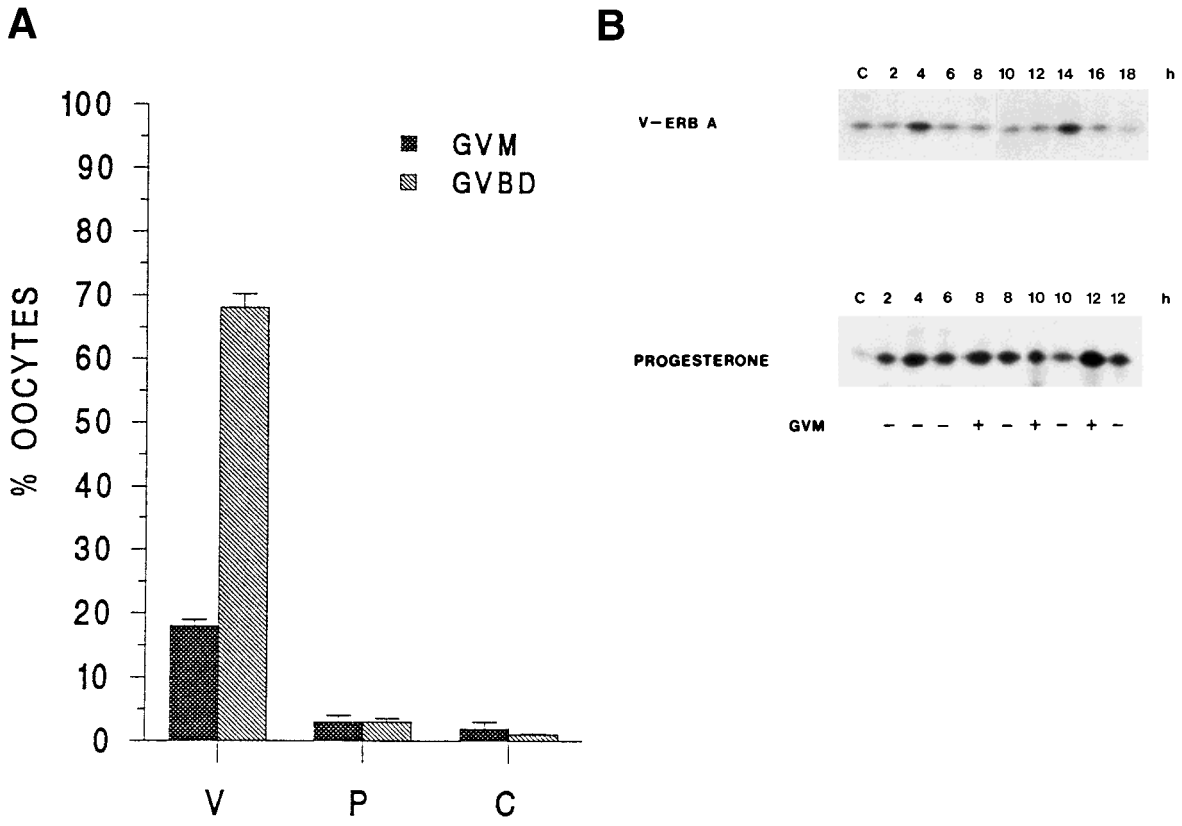

Fig. 2. The effects of expression of v-*erbA* in oocytes occurred independently of the cAMP/MPF pathway. **A:** v-*erbA*–injected (V), *lacZ*-injected (C), or progesterone-treated (P) oocytes were incubated in 20 μM forskolin/2 mM IBMX. After 24 h, the percentage of oocytes displaying GVM was assessed by inspection of whole oocytes, and the frequency of GVBD induction was scored by manual dissection of nuclei in 1% TCA. Three independent experiments were performed (30–40 oocytes per treatment per experiment). The error bars indicate the SEMs. **B:** v-ErbA did not induce MPF histone H1 kinase activity. After microinjection of 5 ng v-*erbA* or pRSV-*lacZ* template as a control (C) (**upper panel**) or incubation in progesterone or O-R2 as a control (C) (**lower panel**), oocytes were collected at the indicated times, and MPF kinase activity was assayed using histone H1 as a substrate and $\gamma[^{32}P]$ ATP. Samples were resolved by 12% SDS-polyacrylamide gel electrophoresis followed by autoradiography. MPF histone H1 kinase activity was assayed in oocytes with (+) or without (−) a distinct white spot (GVM). A representative example of three independent experiments, using oocytes from different female *Xenopus,* is shown.

cytes obtained from the same females. We have shown previously that v-ErbA, synthesized from a microinjected gene template in *Xenopus* oocytes, is functional and acts as a dominant repressor of TR [Nagl et al., 1995]. Microinjection of v-*erbA* expression plasmid into the nucleus of stage VI oocytes resulted in GVM and concomitant pigment displacement which, in most cases, was highly similar in appearance to GVM induced by progesterone after 24 h (Fig. 1A; cf. panels b,c). Occasionally, pigment aggregation in the center of the whitish circular spot in v-*erbA*–injected oocytes was seen (Fig. 1A, panel d). GVM occurred in 41% of v-*erbA*–injected oocytes, while the mean frequency of GVM in progesterone-stimulated oocytes was 69% (Fig. 1B). Next, oocytes were assessed for GVBD and were scored positive when the nucleus could not be dissected intact due to nuclear instability 24 h after microinjection of v-*erbA* template or due to nuclear dissolution after a 24 h incubation in progesterone. According to this criterion, GVBD occurred at a mean frequency of 67% in v-*erbA*–injected oocytes compared to 94% in progesterone-treated oocytes (Fig. 1B). It has been noted previously that the pigment displacement associated with GVM is not always apparent during maturation [Smith, 1989; Bement and Capco, 1990]. In the present study, GVBD could be observed in the absence of GVM both in progesterone-treated and v-*erbA*–injected oocytes.

It should be noted that progression through meiosis, induced by progesterone, occurred at a decelerated pace in all oocytes employed in this study [for comparison see Smith, 1989; Bement and Capco, 1990]. We attribute this fact to seasonal and dietary factors in *Xenopus* donor animals. Since this time course was consistent throughout the study, this did not interfere with the temporal comparison of progesterone- and v-*erbA*–induced events. Progesterone-treated oocytes, scored positive for GVBD, still retained remaining fragments of the germinal vesicle after 24 h. In contrast, when v-*erbA*–injected oocytes were incubated in progesterone, the complete disappearance of the nucleus was observed in all oocytes examined upon manual dissection after 24 h (data not shown). This shortened time course for the complete breakdown of the nucleus may suggest synergistic action of v-ErbA and progesterone in meiotic maturation.

To test whether the partial release of G_2 arrest by v-ErbA required de novo gene expression, we scored the frequency of GVBD in oocytes that had been injected with in vitro–synthesized v-*erbA* protein into the cytoplasm or treated with progesterone and incubated in actinomycin D. Consistent with the reported lack of requirement for gene transcription during progesterone-mediated meiotic induction [Baltus et al., 1973; Sagata et al., 1988; Yew et al., 1992; Sheets et al., 1995], actinomycin D did not affect the frequency of GVBD in progesterone-treated oocytes (data not shown). Since v-*ErbA* was not purified from the translation reaction mixture, it was possible that the rabbit reticulocyte lysate could supply factors that would effect GVBD. Thus, oocytes were injected with lysate mixture as a control. As shown in Figure 1C, the lysate alone did not induce GVBD. Twenty-four hours after microinjection, the mean frequency of GVBD in oocytes injected with v-ErbA and incubated in the absence of inhibitor was 61% in this series of experiments (Fig. 1C). In contrast, incubation of v-ErbA–injected oocytes in actinomycin D reduced the frequency of GVBD to 7.5% (Fig. 1C), showing that the nuclear migration and nuclear instability induced by v-ErbA were dependent on de novo gene expression. A requirement for translation of the newly transcribed message(s) was shown by reduction of GVBD frequency to the same level (i.e., 7.5%), by cycloheximide (data not shown).

Induction of GVM and GVBD by v-ErbA Does Not Involve Activation of the cAMP/MPF Pathway

Treatment of oocytes with forskolin, an adenylate cyclase activator, or IBMX, an inhibitor of cAMP breakdown, blocks meiotic induction by progesterone [reviewed in Smith, 1989; Bement and Capco, 1990]. Forskolin and IBMX did not significantly affect GVBD in v-*erbA*–injected oocytes and decreased GVM only moderately while completely inhibiting progesterone-induced GVM and GVBD (Fig. 2A). MPF kinase activation, the definitive parameter of MPF-mediated oocyte maturation, can be measured in vitro by means of kinase activity of oocyte extracts using histone H1 as a substrate [Langan et al., 1989]. We assayed H1 histone kinase activity in v-*erbA*–injected and progesterone-incubated oocytes in three independent ex-

periments with oocytes obtained from different female *Xenopus*. The results of a representative experiment, using oocytes from the same female, are shown in Figure 2B. Marked v-*erbA*–induced nuclear changes, consistent with the onset of maturation, were present 16 h after microinjection (see Figure 3). Therefore, H1 histone kinase activity was assayed over an 18 h period which included and extended beyond the window of potential MPF activation at the start of maturation. In extracts prepared from v-*erbA*–microinjected oocytes, H1 kinase was not activated over this 18 h period when compared with an extract from *lacZ*-injected controls assayed after 2 h (Fig. 2B). The slightly elevated levels of H1 histone kinase activity in samples assayed 4 h and 14 h after microinjection were interpreted as not significant, as they were not reproduced in repeat assays. Moreover, similar fluctuations in H1 histone kinase activity were also observed in extracts of *lacZ*-injected controls assayed over time (data not shown). Compared with a control extract from oocytes cultured in O-R2, extracts from oocytes incubated in progesterone exhibited high levels of histone H1 kinase activity after 2 h (2 h, GVM−), approximately 6 h prior to the appearance of the white spot (8 h, GVM+) (Fig. 2B). Both in the presence and absence of GVM, strong H1 histone kinase activity was present in extracts from progesterone-incubated oocytes over the entire time interval assayed, except for the extract from oocytes lacking a meiotic spot after a 10 h incubation (10 h, GVM−). In summary, these experiments showed that induction of nuclear migration and nuclear instability in the presence of v-ErbA did not involve the activation of the cAMP-regulated CDC2/MPF pathway.

v-ErbA Initiated Changes in the Nucleus and Cortex Characteristic of Early and Intermediate Meiotic Events

Many studies have relied solely on inspection of whole oocytes and dissection of nuclei to assay for GVM and GVBD, respectively. However, this approach does not allow the distinction of complete maturation from arrested meiosis which is also accompanied by nuclear migration and destabilization [Baltus et al., 1973; Steinert et al., 1974]. To enable us to discriminate between these two outcomes in v-*erbA*–injected oocytes, we performed a detailed analysis of semithin sections from v-*erbA*–injected oocytes exhibiting nuclear instability by differential interference contrast microscopy. As shown in Figure 3A, extensive invaginations of the basal nuclear membrane and lamina were visible in v-*erbA*–expressing oocytes 16 h after microinjection. At 36 h, the invaginations appeared as sealed off lacunae of cytoplasm separated by stretches of nuclear membrane, and a yolk-free area was visible in the cytoplasm below (Fig. 3B). The appearance of v-*erbA*–injected oocytes 36 h after microinjection was highly similar to the appearance of progesterone-treated oocytes after 16 h (Fig. 3D). The dynamic rearrangements of the nuclear membrane in v-*erbA*–injected oocytes eventually resulted in membrane rupture at the apical (animal) pole after 42 h (Fig. 3C), and meiotic spindle formation did not occur. In contrast, in progesterone-induced maturation the rupture of the nucleus always occurs in the vegetal half [Baltus et al., 1973; Bement and Capco, 1990; Hausen and Riebesell, 1991]. Further, in progesterone-treated oocytes meiotic spindle formation was observed after 26 h (data not shown). Apical membrane rupture was not observed in *lacZ*-injected controls, demonstrating that rupture in v-*erbA*–injected oocytes was not due to damage during the process of microinjection (Fig. 3E). Nuclear membrane rupture at the apex has previously been shown to be independent of the site of oocyte microinjection and is associated with arrested meiotic maturation [Baltus et al., 1973; Steinert et al., 1974].

The progressive ultrastructural changes taking place in the nucleus and the cytoplasm during maturation have been well characterized [Bement and Capco, 1990] and can serve as markers for temporal subsets of meiotic transformations. As shown in Figure 4A, the vegetal half of the nucleus in *lacZ*-injected controls was extensively folded, forming narrow cytoplasmic channels and larger invaginations extending into the nucleoplasm. Annulate lamellae (AL) were often seen in the cytoplasm, in close proximity to the nuclear membrane. *LacZ*-injected oocytes were identical in appearance to uninjected oocytes (data not shown). In contrast, in v-*erbA*–injected oocytes, the structure of the nuclear membrane was drastically altered. v-ErbA induced the formation of long stretches of adjoined double membranes and the transformation of AL into cisternae (Fig. 4B–E). Seen in

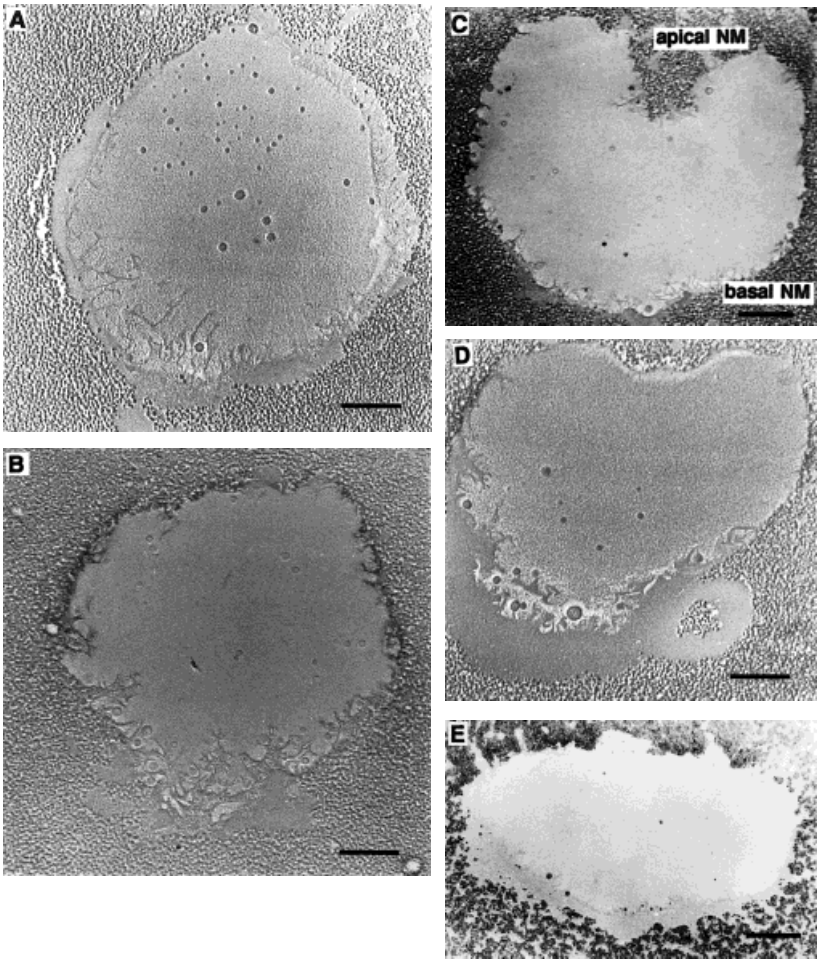

Fig. 3. Semithin sections of nuclei of v-*erbA*–expressing oocytes showed structural changes indicative of meiotic induction, but meiosis was arrested prior to spindle formation. **A:** Invaginations of the basal nuclear membrane and lamina in v-*erbA*–expressing oocytes 16 h after microinjection. **B:** Progressive v-ErbA–mediated structural changes along the circumference of the nuclear membrane and yolk-free zone below the basal nuclear membrane 36 h after microinjection. **C:** Rupture of the apical nuclear membrane (NM) in v-*erbA*–expressing oocytes 42 h after microinjection. **D:** Invaginations of the basal nuclear membrane and lamina and yolk-free space in progesterone-induced oocytes after 16 h. **E:** Absence of nuclear membrane invaginations in *lacZ*-injected control oocytes 36 h after microinjection. Scale bars = 100 μM.

cross-section, the two double membranes appeared tightly adjoined to each other, except for small islands of enclosed cytoplasmic material (Fig. 4D,E). A striking feature of this membrane rearrangement was the alignment of nuclear pore complexes (NPCs) across the joined membranes (Fig. 4F). Furthermore, clustering of NPCs, with adjacent portions of nuclear membrane depleted of NPCs, was seen in the basal regions of the nuclear envelope (Fig. 4G,H). Concomitant with the altered nuclear membrane architecture, multiple layers of cisternae devoid of NPCs developed (Fig. 4I). In addition, the nucleoli showed signs of meiotic transformation (Fig. 4J); that is, the granular and fibrillar parts had become clearly segregated. The rearrangements of the basal nuclear membrane, NPC clustering, AL transformation into cisternae, and segregation of the granular and fibrillar components of nucleoli represent the initiation of events leading to the disassembly of the nuclear membrane and NPCs during meiosis [Bement and Capco, 1990; Brachet et al., 1970; Steinert et al., 1974; Kessel and Subtelny, 1981].

The cortex of oocytes expressing v-*erbA* exhibited a subset of meiotic changes but did not develop the characteristics belonging to the late stage of maturation (Fig. 5A–C). Microvilli, although less numerous and shortened compared to untreated controls (data not shown), were present 36 h after microinjection of v-*erbA* template (Fig. 5A,C), whereas they were lacking

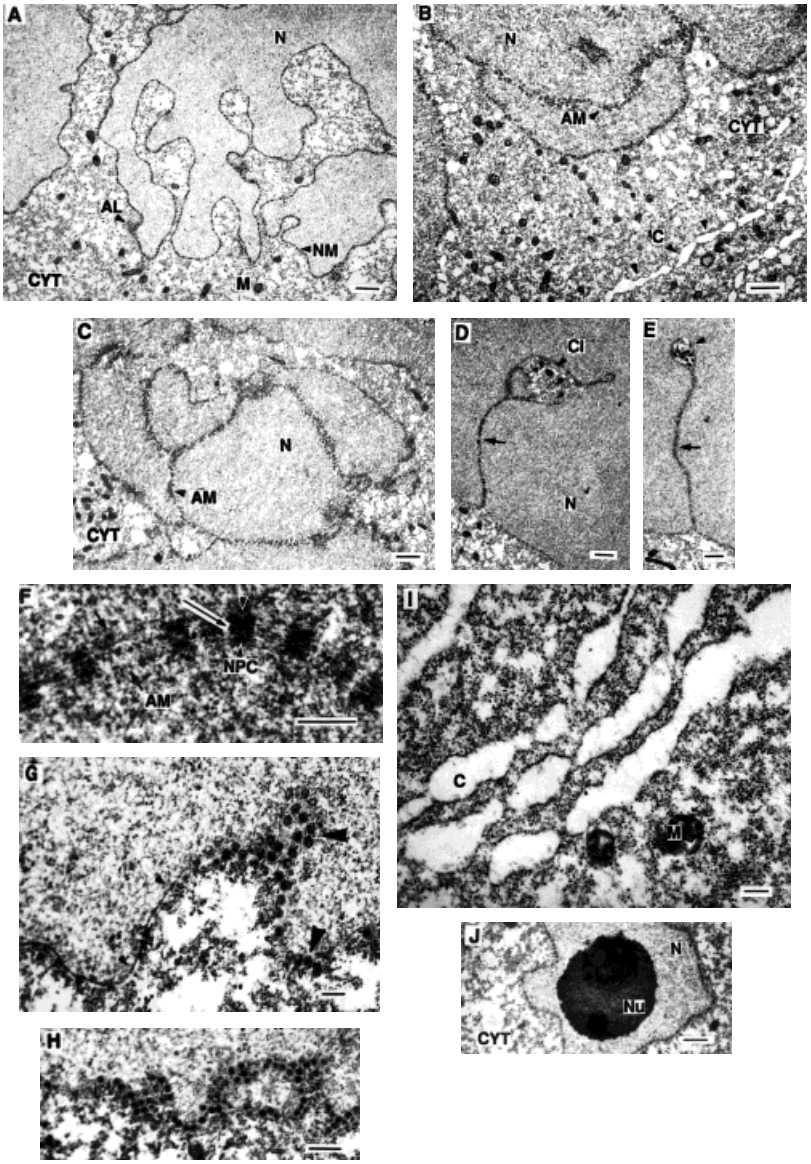

Fig. 4. Ultrastructural meiotic changes in thin sections of nuclei of v-*erbA*–expressing oocytes. **A:** The basal nuclear membrane (NM) of control oocytes injected with 5 ng *lacZ* template was highly folded and formed narrow channels of cytoplasm (CYT) and lobes extending into the nucleus (N). Annulate lamellae (AL) are visible close to the nuclear membrane (en face view). M, mitochondrion. **B–J:** Thin sections of v-*erbA*–expressing oocytes. B,C: Extensive regions of nuclear membrane were tightly adjoined to each other 36 h after microinjection (adjoined membranes, AM). AL had become transformed into cisternae (C). CYT, cytoplasm; N, nucleus. D,E: Long stretches of adjoined membranes (arrows) with aligned NPCs (arrowheads) separated off islands of cytoplasm (CI) containing mitochondria and other cytoplasmic material. N, nucleus. F: NPCs (arrowheads) were aligned across the adjoined membranes (short arrows) by electron-dense material (long arrow). AM, adjoined membranes. G,H: NPCs in the basal nuclear membrane were clustered (large arrowheads), with adjacent regions being depleted of NPCs (small arrowheads), 36 h after microinjection. I: AL were transformed into cisternae (C) devoid of NPCs. M, mitochondrion. J: The nucleoli (Nu) were segregated into distinct fibrillar and granular regions. CYT, cytoplasm; N, nucleus. A–E,J: Scale bars = 1 μm. H: Scale bar = 500 nm. F,G,I: Scale bar = 200 nm.

after 16 h in oocytes undergoing progesterone-induced maturation (Fig. 5D). Pigment granules were clustered at a distance from the plasma membrane in both v-*erbA*–expressing (Fig. 5B) and progesterone-induced oocytes (Fig. 5E), resulting in formation of a whitish circular spot. In contrast, the majority of cortical granules in v-*erbA*–expressing oocytes remained localized adjacent to the plasma membrane in the area of displaced pigment (Fig. 5B) but were retracted into the interior in progesterone-treated oocytes (Fig. 5E,F). This finding is con-

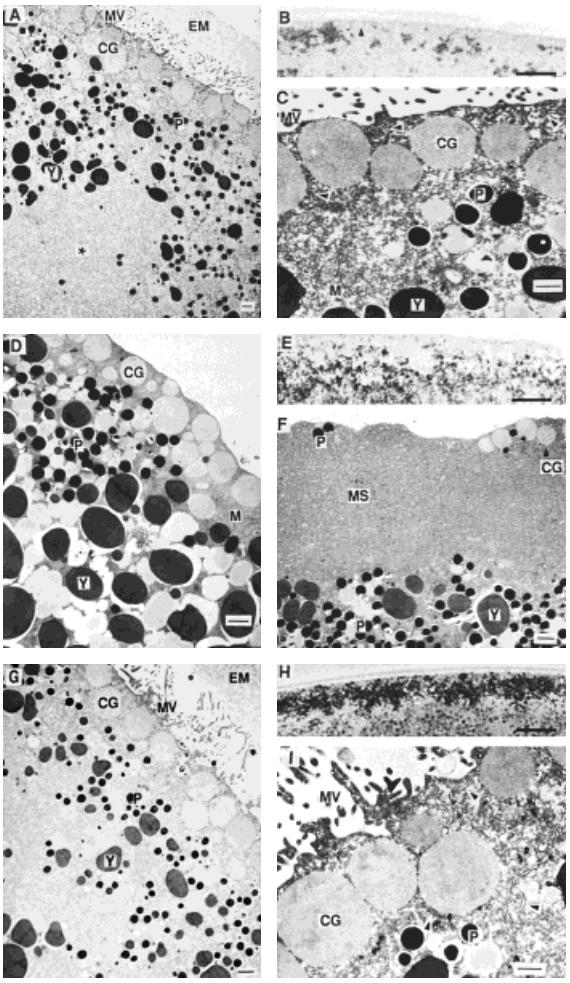

Fig. 5. The cortex of v-*erbA*–expressing oocytes showed a subset of meiotic transformations in thin and semithin sections. **A:** In the cortex of v-*erbA*–expressing oocytes, microvilli (MV) and yolk-free corridors (asterisk) were visible 36 h after microinjection. Cortical granules (CG) were localized immediately below the plasma membrane. EM, extracellular matrix; P, pigment granules; Y, yolk platelet. **B:** Pigment granules were retracted and clustered in the cytoplasm, while cortical granules (arrowhead) were present adjacent to the apical plasma membrane, in the area of the displaced pigment 36 h after microinjection of v-*erbA* (semithin section). **C:** The microvilli of v-*erbA*–expressing oocytes were partially retracted and of low density. The cortical endoplasmic reticulum (arrowheads) had not formed an extensive network and did not encircle the cortical granules. CG, cortical granules; M, mitochondrion; MV, microvilli; P, pigment granules; Y, yolk platelet. **D:** Progesterone-induced maturation resulted in the complete retraction of microvilli after 16 h; yolk-free corridors were disrupted, and mitochondria (M) were randomly dispersed throughout the cortex. CG, cortical granules; P, pigment granules; Y, yolk platelet. **E:** Progesterone induction caused the retraction of cortical granules and the clustering of pigment granules in the cytoplasm (semithin section). **F:** Retraction of almost all cortical granules (CG), pigment granules (P), and other vesicles resulted in an area of clear cytoplasm in the meiotic white spot (MS) of progesterone-induced oocytes after 16 h. Y, yolk platelet. **G:** Cortex of a *lacZ*-injected control oocyte 36 h after microinjection. CG, cortical granules; EM, extracellular matrix; MV, microvilli; P, pigment granules; Y, yolk platelets. **H:** Continuous pigment layer adjacent to the plasma membrane in a *lacZ*-injected oocyte 36 h after microinjection (semithin section). **I:** Numerous extended microvilli (MV) in a *lacZ*-injected oocyte 36 h after microinjection. The cortical endoplasmic reticulum (arrowheads) was comparable to that of v-*erbA*–injected oocytes. CG, cortical granules; P, pigment granules. A: Scale bar = 2 μm. B,E,H: Scale bars = 100 μm. D,F,G: Scale bars = 1 μm. C,I: Scale bars = 500 nm.

sistent with the observation that the rapid decrease in cAMP level triggered by progesterone correlates with the movement of cortical granules away from the plasma membrane, suggesting that cortical granule position is controlled by the level of intracellular cAMP [Bement and Capco, 1990]. Since v-ErbA–induced changes occur without a decrease in cAMP, the cortical

granules would be expected to remain at the plasma membrane. In oocytes microinjected with the *lacZ* plasmid, microvilli were more numerous and further extended (Fig. 5G,I) than in v-*erbA*–injected oocytes (Fig. 5A,C). The layer of pigment granules was continuous in *lacZ*-injected oocytes and located directly adjacent to the plasma membrane (Fig. 5H), differing markedly from the clustered pigment arrangement in v-*erbA*–injected oocytes (Fig. 5B). The structure of the cortical endoplasmic reticulum in *lacZ*-injected controls (Fig. 5I) was comparable to that of the cortical endoplasmic reticulum in v-*erbA*–expressing oocytes (Fig. 5C). Finally, features characteristic of late meiotic maturation—for example, disruption of the yolk-free corridors and development of an extensive cortical endoplasmic reticulum—were not seen in v-*erbA*–expressing oocytes (Fig. 5A,C). A summary of the comparison of ultrastructural changes induced by progesterone and v-ErbA is presented in Table I.

TABLE I. Induction of Early and Intermediate Meiotic Events by v-ErbA in *Xenopus* Oocytes

Meiotic event[a]	v-ErbA[b]
Early	
AL transformation	+
Basal membrane changes	+
Cortical granule retraction	−
Intermediate	
Nuclear migration	+
Pigment rearrangement	+
NPC repositioning	initiated
Nucleolar dissolution	initiated
Microvilli retraction	initiated
GVBD	apical breakdown
Chromosome condensation	−
Late	
Yolk-free corridor disruption	−
AL absent	−
Cortical ER development	−
Microvilli retraction completed	−
Meiotic spindle	−

[a]Meiotic events were timed [Bement and Capco, 1990] and identified as described [Bement and Capco, 1990; Hausen and Riebesell, 1991; Brachet et al., 1970; Steinert et al., 1974; Kessel and Subtelny, 1981; Kessel, 1992].
[b]The presence (+) or absence (−) of events indicative of different stages of progesterone-induced maturation, in v-*erbA*–expressing oocytes is shown (see Figs. 4, 5).

v-ErbA Did Not Act as a Dominant Antagonist of Endogenous TR

Some of the growth-promoting properties of v-ErbA in mammalian cells are mediated by dominant repression of TR and RAR [Sharif and Privalsky, 1991; Desbois et al., 1991a,b; Zhang et al., 1991; Gandrillon et al., 1994]. Stage VI *Xenopus* oocytes contain low levels of TRα and TRβ protein [Eliceiri and Brown, 1994] but lack thyroid hormone [Nagl et al., 1995]. Conceivably, unliganded TR might contribute to the G_2 arrest by repressing certain M-phase–inducing genes. Therefore, we wished to assess whether dominant negative inactivation of unliganded TR by v-ErbA was responsible for the induction of early meiotic events. We have shown elsewhere that the action of endogenous oocyte TR can be blocked by a dominant negative in vitro–generated mutant of human TRβ (TR C122 > A) [Nagl et al., 1995]. When v-ErbA was replaced by the mutant TR C122 > A, the morphology of the basal nuclear membrane in TR C122 > A–injected oocytes was identical to that of untreated G_2-arrested oocytes (Fig. 6). This finding suggests that v-ErbA–induced ultrastructural changes, characteristic of early and intermediate maturation events, were not initiated by v-ErbA acting as a dominant antagonist of endogenous TR.

v-ErbA Was Detectable at Nuclear Pore Complexes

In immunoprecipitation assays, v-ErbA, synthesized in oocytes, is almost exclusively recovered from manually isolated nuclei, while approximately 10% of v-ErbA partitions to the cytoplasmic fraction (data not shown). In oocyte fractionation assays, a protein with a molecular weight of approximately 75 kD was detectable in total soluble protein fractions from isolated nuclei 8 h after microinjection of the gene template (Fig. 7A, panel a). This protein corresponds in size to the full-length *gag*-v-*erbA* fusion protein encoded by the RS-v-*erbA* expression template [Privalsky, 1992]. After 24 h, accumulation of the 75 kD protein in nuclear fractions was further increased, and, surprisingly, the protein was also detectable in total soluble protein fractions from isolated nuclear membranes (Fig. 7A, panel b). To confirm the identity of the 75 kD protein, we carried out immunoprecipitation assays on both fractions using a monoclonal antibody with dual specificity for both v-*erbA* and chicken c-*erbA* [Freake et al.,

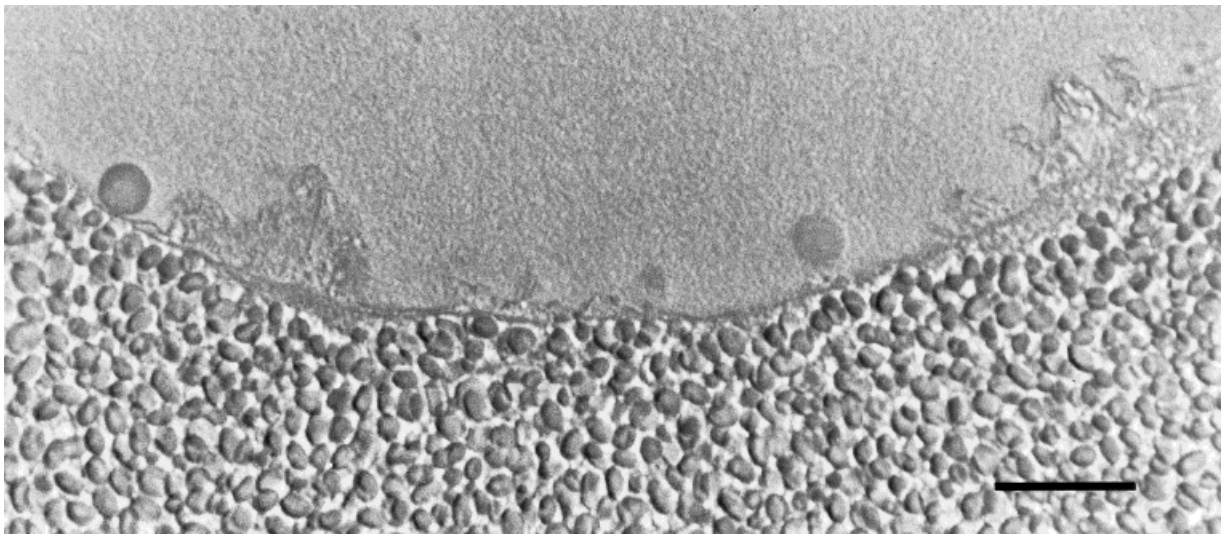

Fig. 6. A dominant negative mutant of TR did not mimic the action of v-ErbA. Semithin section showing the basal nuclear membrane of a TR C122 > A–injected oocyte 36 h after microinjection. Scale bar = 20 μm.

1988]. As shown in Figure 7A, panel c, the 75 kD protein was immunoprecipitated from the nuclear membrane and nuclear fractions. In contrast, deliberate overexposure of the fluorograph showed that wild-type chicken c-ErbA, expressed from injected c-*erbA* templates, was exclusively immunoprecipitated from the nuclear fraction (Fig. 7A, panel d).

To identify the precise location of v-ErbA, we performed immunogold labeling of manually isolated nuclear membranes (Fig. 7B). Nuclear membranes, isolated from v-*erbA*–expressing oocytes, were exclusively decorated with gold particles at the cytoplasmic face of NPCs (Fig. 7B, panels a–c), and, more specifically, the v-*erbA* product was localized to the fibrils emanating from the cytoplasmic annuli (Fig. 7B, panels d,e). A possible reason for the relatively low labeling density, which contrasted with the strong signal obtained by immunoprecipitation, is that the primary antibody was raised against a synthetic peptide of v-*erbA* (residues 58–75) within the DNA binding domain. Since the DNA binding domain is separated from the v/c-*erbA* nuclear localization sequence (NLS) by only 12 amino acid residues [LaCasse and Lefebvre, 1995], antibody accessibility might have been reduced due to steric hindrance caused by interactions between the NLS and a NPC component(s). Control nuclear membranes from uninjected oocytes did not exhibit immunogold labeling with the anti-*erbA* antibody (data not shown), indicating that the observed binding of the gold probes to the cytoplasmic fibrils was specific for the v-ErbA antigen.

DISCUSSION

Our study shows that v-ErbA induces ultrastructural changes in *Xenopus* oocytes characteristic of early and intermediate events of meiosis. This subset of meiotic events was induced by v-ErbA independently of the cAMP-regulated CDC2/MPF pathway and required gene transcription. Importantly, a dominant negative mutant of TR did not induce ultrastructural changes in oocytes, suggesting that this effect of v-ErbA was not mediated by inactivating endogenous TR. This finding implies the existence of a pathway for the partial release of the G_2 arrest in oocytes which can be triggered by the expression of an as yet unidentified v-ErbA–inducible gene(s). The identification of this gene(s) can be expected to provide further insights into the mechanisms through which v-ErbA promotes cell growth.

The rearrangements of the basal nuclear membrane, NPC clustering, annulate lamellae transformation into cisternae, and segregation of the granular and fibrillar components of nucleoli, which were all observed in v-*erbA*–expressing oocytes, represent the initiation of events leading to the disassembly of the nuclear membrane and NPCs during meiosis [Bement and Capco, 1990; Brachet et al., 1970; Steinert et al., 1974; Kessel and Subtelny, 1981]. However, the reorganization of the nuclear mem-

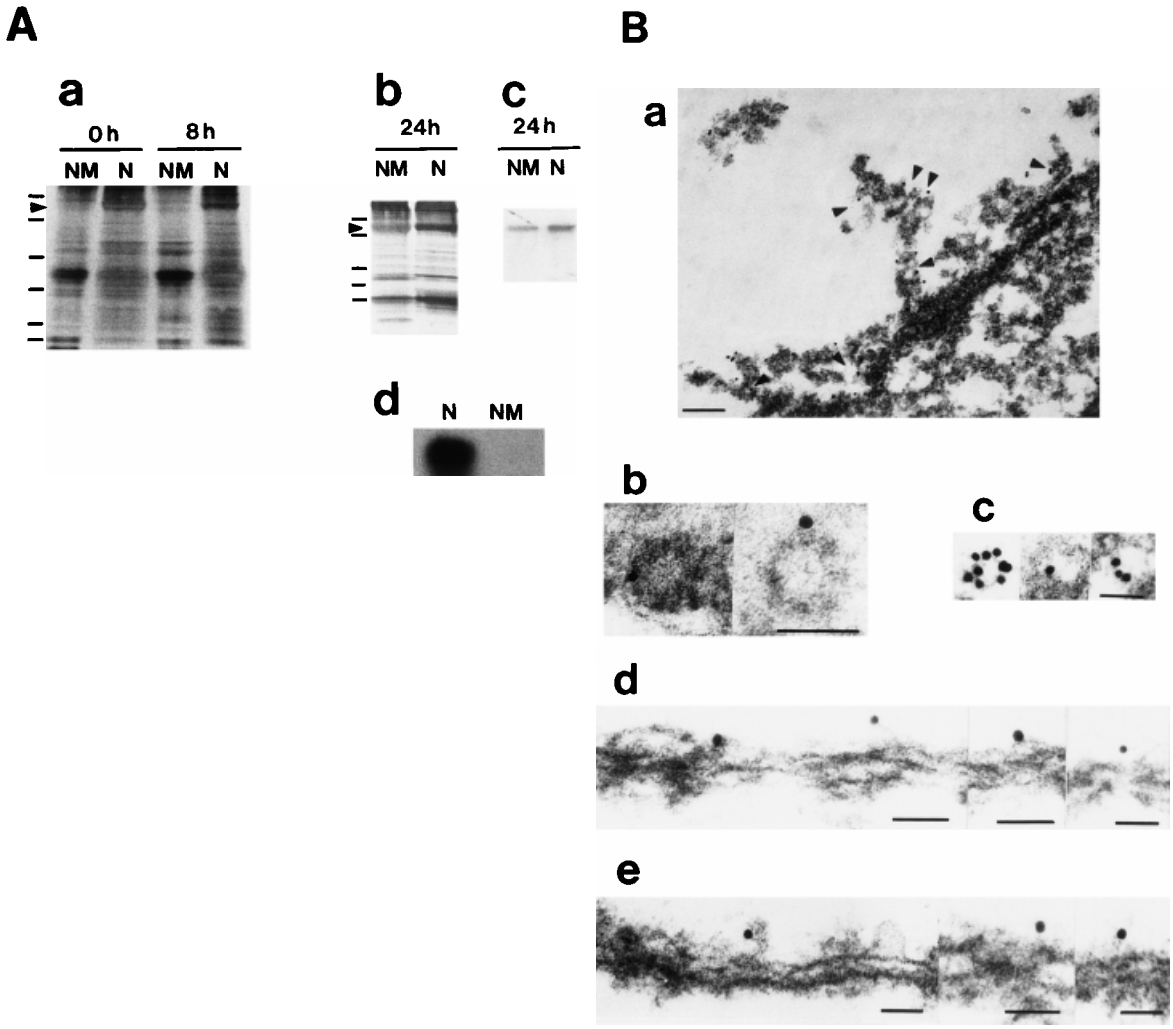

Fig. 7. v-ErbA was detectable at nuclear pores. **A:** Low amounts of v-ErbA were present in nuclear membrane fractions. **Panel a:** Total soluble protein fractions were prepared from ten manually isolated nuclei (N) or nuclear membranes (NM) 0 or 8 h after microinjection of 5 ng v-*erbA* expression template and resolved by 12% SDS-PAGE and silver staining. The arrowhead indicates a protein of approximately 75 kD, corresponding in size to the full-length *gag*-v-*erbA* fusion protein. Molecular weights (D) are indicated by dashes: 85,200, 55,600, 39,200, 26,600, 20,100, and 14,300. **Panel b:** Total soluble protein fractions from ten nuclei or ten nuclear membranes 24 h after microinjection. Symbols are as described in panel a. **Panel c:** The 75 kD *gag*-v-*erbA* protein was immunoprecipitated from nuclear membrane and nuclear fractions using anti-v/c-*erbA* antibodies. Oocytes microinjected with 5 ng v-*erbA* expression vector were cultured in O-R2 medium with 1 mCi/ml L-[^{35}S] methionine for 24 h, and nuclear membranes and nuclei were manually isolated. Nuclear membrane (NM) and nuclear (N) fractions of ten v-*erbA*–injected oocytes were incubated with protein G–Sepharose-antibody complexes in an immunoprecipitation assay. Labeled polypeptides were recovered and separated by 12% SDS-PAGE followed by fluorography. **Panel d:** c-ErbA was exclusively immunoprecipitated from the nuclear fraction. Immunoprecipitation of c-*erbA* protein from the nuclear (N) and nuclear membrane (NM) fractions of 20 oocytes injected with 5 ng c-*erbA* expression vector was carried out as described in panel c. **B:** Immunogold EM detection of v-ErbA at NPCs. Manually isolated nuclear membranes from v-*erbA*–injected oocytes were immunolabeled with 10 nm colloidal gold using a v-*erbA*-specific monoclonal antibody in a biotin-streptavidin bridging technique prior to embedding and thin sectioning. **Panel a:** An en face view of the cytoplasmic side of the nuclear envelope. Arrowheads indicate examples of colloidal gold–labeled NPCs clearly revealed by this plane of sectioning. **Panels b,c:** Selected examples of transversely sectioned NPCs labeled by the anti-v-*erbA* antibody. **Panels d,e:** Representative examples of tangentially sectioned nuclear envelopes. The v-*erbA*–specific antibody exclusively labeled the cytoplasmic fibrils of NPCs. The cytoplasmic side of all cross-sectioned nuclear envelopes faces the top of the figure. The cytoplasmic side of the nuclear envelope often forms blebs (panel e). a: Scale bar = 200 nm. b: Scale bar = 100 nm. c–e: Scale bar = 50 nm.

brane in v-*erbA*–injected oocytes did not proceed past this intermediate stage, and eventually the nuclear membrane ruptured at the apical pole. CDC2/MPF, either directly or through activation of other protein kinases, induces disassembly of the nuclear lamina filaments and NPCs and the vesicularization of the nuclear membrane [reviewed in Smith, 1989; Bement and Capco, 1990], and chromosome condensation and meiotic spindle formation are mediated by the reorganization of microtubules by CDC2/MPF and MAPK [Smith, 1989; Bement and Capco, 1990]. The failure of these progressive events to occur in v-*erbA*–expressing oocytes was correlated with the fact that CDC2/MPF was not activated and that v-ErbA–mediated nuclear changes were not inhibited by taxol. This suggests that the nuclear changes did not involve rearrangements of the microtubular network and, by implication, occurred independently of an MPF/MAPK requirement.

There was a striking match between the v-*erbA*–induced events and oocyte pseudomaturation [Smith, 1989; Baltus et al., 1973; Steinert et al., 1974]. In pseudomaturation, a distinctive subset of structural changes is induced in the absence of MPF activation and de novo synthesis of c-*mos* protein [Drury and Schorderet-Slatkine, 1975; Wasserman and Masui, 1975; Kobayashi et al., 1991]—in particular, adjoined nuclear membranes, mottling of the pigment layer, and condensation of the fibrillar core of the nucleoli [Baltus et al., 1973; Steinert et al., 1974]. Moreover, spindle formation is never observed in pseudomaturation, and eventually apical rupture of the nuclear membrane occurs [Brachet et al., 1970; Steinert et al., 1974; Drury and Schorderet-Slatkine, 1975]. In oocytes, M-phase induction by v-ErbA, like pseudomaturation, is ultimately a destructive process. The reason for this most likely lies in the absence of additional signals from activated protein kinases, essential for the completion of maturation. Once the G_2/M restriction point is passed, the maturing oocyte is committed to undergo events leading to GVBD and lacks the ability to reverse the meiotic pathway. Consequently, the initiated structural transformations eventually lead to the disintegration of the oocyte. This situation is wholly different from the context in which v-ErbA functions in somatic cells. Somatic cells constantly receive a wide range of extracellular signals conveyed by growth factors, which activate mitogenic kinases. Abnormal activation of a gene(s), encoding a putative cell cycle inducer, by v-ErbA can be expected to act in a complementary manner to these events and to enhance certain mitogenic signals. As a result, v-ErbA apparently does not cause nuclear dissolution in somatic cells but confers a reduced requirement for growth factors and an enhanced growth potential [Gandrillon et al., 1987].

In summary, the partial release of G_2 arrest by v-ErbA appears to allow meiotic ultrastructural transformation up to a point where signal transmission by activated MPF and the subsequent phosphorylation cascade become essential for M-phase progression. In somatic cells, v-ErbA cooperates with oncogenic tyrosine kinases, such as v-*erbB*, v-*src*, or v-*sea*, to achieve a fully transformed phenotype [Frykberg et al., 1983; Kahn et al., 1986; Schroeder et al., 1992]. The effects of v-ErbA in initiating the partial release from G_2 arrest in oocytes may be seen as corresponding to the strictly cooperative role of the v-*erbA* oncogene in cellular transformation.

A portion of v-ErbA expressed in oocytes was present at the nuclear membrane at the cytoplasmic face of the NPCs near the cytoplasmic annuli. Specifically, colloidal gold–labeled v-ErbA was detected at the cytoplasmic fibrils of the NPCs, possibly at fibril components, which have been shown to be involved in NLS-mediated ligand docking [Forbes, 1992; Görlich et al., 1994]. That components of the nuclear import machinery may interfere with cell cycle regulation is demonstrated by the effects of a mutation in the *S. cerevisiae* NLS receptor, Srp1, that targets proteins to the NPC [Loeb et al., 1995]. A conditional *srp1* mutant arrests cells at the G_2/M border and was suggested to act by blocking the import of a critical cell cycle regulator. Similarly, Pendulin (or *OHO31*), a *Drosophila* tumor suppressor gene product with sequence homology to Srp1, exhibits cell-cycle-dependent nuclear localization and is required for normal cell proliferation [Küssel and Frasch, 1995; Török et al., 1995]. In addition, other recent studies showed that the fibrils emanating from the cytoplasmic face of NPCs contain the proteins CAN/nup214 [Kraemer et al., 1994] and TPR/nup265 [Byrd et al., 1994], which have both been associated with oncogenesis in humans when fused to other genes. Thus, oncogenes may be capable of inducing oncogenesis by altering the functions of NPCs. Potential effects of v-ErbA at NPCs would be expected to

play an early inductive role, as the association of v-ErbA with NPCs occurs well in advance of meiotic events. While the significance of the localization of v-ErbA at NPCs remains to be determined, it is interesting to consider the possibility that in addition to its intranuclear function in gene activation v-ErbA might modulate nucleocytoplasmic transport of a key cell cycle regulator(s).

ACKNOWLEDGMENTS

This work was supported in part by research grants from the Cancer Society, Lottery Health Research, and Health Research Council of New Zealand (to L.A. Allison). S.B. Nagl was the recipient of a predoctoral scholarship from the Ministry of Research, Science and Technology of New Zealand and a New Zealand Universities' postgraduate scholarship. C.F. Bunn is the recipient of a predoctoral Sargood Bequest Cancer Research Training Scholarship from the New Zealand Cancer Society. We thank J.C. McKenzie for assistance with the light microscopy and EM analysis. We also thank Dr. R.M. Evans for the gift of RS-v-*erbA*, Dr. P.J. Romaniuk for the gift of hTRβ C122 > A, Dr. B. Vennström for the gift of pKCR2-cea, Dr. M. Privalsky for the gift of pGEM-4Z, and Dr. M. Harkey for the gift of pRSV-*lacZ*.

REFERENCES

Allison LA, Romaniuk PJ, Bakken AH (1991): RNA-protein interactions of stored 5S RNA with TFIIIA and ribosomal protein L5 during *Xenopus* oogenesis. Dev Biol 144:129–144.

Allison LA, North MT, Murdoch KJ, Romaniuk PJ, Deschamps S, le Maire M (1993): Structural requirements of 5S rRNA for nuclear transport, 7S ribonucleoprotein particle assembly, and 60S ribosomal subunit assembly in *Xenopus* oocytes. Mol Cell Biol 13:6819–6831.

Baltus E, Brachet J, Hanocq-Quertier J, Hubert E (1973): Cytochemical and biochemical studies on progesterone-induced maturation in amphibian oocytes. Differentiation 1:127–143.

Bement WM, Capco DG (1990): Transformation of the amphibian oocyte into the egg: Structural and biochemical events. J Electron Microsc Tech 16:202–234.

Brachet J, Hanocq F, Van Gansen P (1970): A cytochemical and ultrastructural analysis of in vitro maturation in amphibian oocytes. Dev Biol 21:157–195.

Byrd DA, Sweet DJ, Pante N, Konstantinov KN, Guan T, Saphire ACS, Mitchell PJ, Cooper CS, Aebi U, Gerace L (1994): Tpr, a large coiled coil protein whose amino terminus is involved in activation of oncogenic kinases, is localized to the cytoplasmic surface of the nuclear pore complex. J Cell Biol 127:1515–1526.

Chen H-W, Smit-McBride Z, Lewis S, Sharif M, Privalsky ML (1993): Nuclear hormone receptors involved in neoplasia: ErbA exhibits a novel DNA sequence specificity determined by amino acids outside of the zinc finger region. Mol Cell Biol 13:2366–2376.

Cordes VC, Reidenbach S, Kohler A, Stuurman N, van Driel R, Franke WW (1993): Intracellular filaments containing a nuclear pore complex protein. J Cell Biol 123:1333–1344.

Damm K, Thompson CC, Evans RM (1989): Protein encoded by v-*erbA* functions as a thyroid hormone receptor antagonist. Nature 339:593–597.

Desbois C, Pain B, Guilhot C, Benchaibi M, Ffrench M, Ghysdael J, Madjar J-J, Samarut J (1991a): *v-erbA* oncogene abrogates growth inhibition of chicken embryo fibroblasts induced by retinoic acid. Oncogene 6:2129–2135.

Desbois C, Aubert D, Legrand C, Pain B, Samarut J (1991b): A novel mechanism of action for v-ErbA: Abrogation of the inactivation of transcription factor AP-1 by retinoic acid and thyroid hormone receptors. Cell 67:731–740.

Drury KC, Schorderet-Slatkine S (1975): Effects of cycloheximide on the "autocatalytic" nature of the maturation promoting factor (MPF) in oocytes of *Xenopus laevis*. Cell 4:269–274.

Dumont JN (1972): Oogenesis in *Xenopus laevis* (Daudin) I. Stages of oocyte development in laboratory maintained animals. J Morphol 136:153–180.

Eliceiri BP, Brown DD (1994): Quantitation of endogenous thyroid hormone receptors α and β during embryogenesis and metamorphosis in *Xenopus laevis*. J Biol Chem 269: 24459–24465.

Forbes DJ (1992): Structure and function of the nuclear pore complex. Annu Rev Cell Biol 8:495–527.

Freake HC, Santos A, Goldberg Y, Ghysdael J, Oppenheimer JH (1988): Differences in antibody recognition of the triiodothyronine nuclear receptor and c-erbA products. Mol Endocrinol 2:986–991.

Frykberg L, Palmieri S, Beug H, Graf T, Hayman M, Vennström B (1983): Transforming capacities of avian erythroblastosis virus mutants deleted in the *erbA* or *erbB* oncogenes. Cell 32:227–238.

Gandrillon O, Jurdic P, Benchaibi M, Xiao J-H, Ghysdael J, Samarut J (1987): Expression of the v-*erbA* oncogene in chicken embryo fibroblasts stimulates their proliferation in vitro and enhances tumor growth in vivo. Cell 49:687–697.

Gandrillon O, Ferrand N, Michaille J-J, Roze L, Zile MH, Samarut J (1994): c*erbA*α/T3R and RARs control commitment of hematopoietic self-renewing progenitor cells to apoptosis or differentiation and are antagonized by the v-*erbA* oncogene. Oncogene 9:749–758.

Görlich D, Prehn S, Laskey RA, Hartmann E (1994): Isolation of a protein that is essential for the first step of nuclear protein import. Cell 79:767–778.

Gorman C, Padmanabhan R, Howard BH (1983): High efficiency DNA-mediated transformation of primate cells. Science 221:551–553.

Hausen P, Riebesell M (1991): "The Early Development of Xenopus laevis. An Atlas of Histology." New York: Springer Verlag.

Kahn P, Frykberg C, Brady C, Stanley I, Berg H, Vennström B, Graf T (1986): v-*erbA* cooperates with sarcoma oncogenes in leukemic cell transformation. Cell 45:349–356.

Kessel RG (1992): Annulate lamellae: A last frontier in cellular organelles. Int Rev Cytol 133:43–120.

Kessel RG, Subtelny S (1981): Alteration of annulate lamellae in the in vitro progesterone-treated, full-grown *Rana pipiens* oocyte. J Exp Zool 217:119–135.

Kobayashi H, Minshull J, Ford C, Golsteyn R, Poon R, Hunt T (1991): On the synthesis and destruction of A- and B-type cyclins during oogenesis and meiotic maturation in *Xenopus laevis*. J Cell Biol 114:755–765.

Kosako H, Gotoh Y, Nishida E (1994a): Requirement for the MAP kinase kinase/MAP kinase cascade in *Xenopus* oocyte maturation. EMBO J 13:2131–2138.

Kosako H, Gotoh Y, Nishida E (1994b): MAP kinase cascade in *Xenopus* oocytes. J Cell Sci S18:115–119.

Kraemer D, Wozniak RW, Blobel G, Radu A (1994): The human CAN protein, a putative oncogene product associated with myeloid leukemogenesis, is a nuclear pore complex protein that faces the cytoplasm. Proc Natl Acad Sci U S A 91:1519–1523.

Krohne G, Franke WW (1983): Proteins of pore complex–lamina structures from nuclei and nuclear membranes. Methods Enzymol 96:597–608.

Küssel P, Frasch M (1995): Pendulin, a *Drosophila* protein with cell cycle–dependent nuclear localization, is required for normal cell proliferation. J Cell Biol 129:1491–1507.

LaCasse EC, Lefebvre YA (1995): Nuclear localization signals overlap DNA- or RNA-binding domains in nucleic acid–binding proteins. Nucleic Acids Res 23:1647–1656.

Langan TA, Gautier J, Lohka M, Hollingsworth R, Moreno S, Nurse P, Maller J, Sclafani RA (1989): Mammalian growth-associated histone H1 kinase: A homolog of *cdc2*$^+$/*CDC28* protein kinase controlling mitotic entry in yeast and frog cells. Mol Cell Biol 9:3860–3868.

Loeb JDJ, Schlenstedt G, Pellman D, Kornitzer D, Silver PA, Fink GR (1995): The yeast nuclear import receptor is required for mitosis. Proc Natl Acad Sci U S A 92:7647–7651.

Maller JL (1990): *Xenopus* oocytes and the biochemistry of cell division. Biochemistry 29:3157–3166.

Mordret G (1993): MAP kinase kinase: A node connecting multiple pathways. Biol Cell 79:193–207.

Nagl SB, Nelson CC, Romaniuk PJ, Allison LA (1995): Constitutive transactivation by the thyroid hormone receptor and a novel pattern of activity of its oncogenic homolog v-*ErbA* in *Xenopus* oocytes. Mol Endocrinol 9: 1522–1532.

Nelson CC, Faris JS, Hendy SC, Romaniuk PJ (1993): Functional analysis of the amino acids in the DNA recognition α-helix of the human thyroid hormone receptor. Mol Endocrinol 7:1185–1195.

Privalsky ML (1992): v-*erb A*, nuclear hormone receptors, and oncogenesis. Biochim Biophys Acta 1114:51–62.

Sagata N, Oskarsson M, Copeland T, Brumbaugh J, Vande Woude GF (1988): Function of c-*mos* proto-oncogene product in meiotic maturation in *Xenopus* oocytes. Nature 335:519–525.

Sap J, Munoz A, Schmitt J, Stunnenberg H, Vennström B (1989): Repression of transcription mediated at a thyroid hormone response element by the v-*erbA* oncogene product. Nature 340:242–244.

Schroeder C, Gibson L, Beug H (1992): The v-*erb*A oncogene requires cooperation with tyrosine kinases to arrest erythroid differentiation induced by ligand-activated endogenous c-*erb*A and retinoic acid receptor. Oncogene 7:203–216.

Sharif M, Privalsky ML (1991): v-*erb A* oncogene function in neoplasia correlates with its ability to repress retinoic acid receptor action. Cell 66:885–893.

Sheets MD, Wu M, Wickens M (1995): Polyadenylation of c-*mos* mRNA as a control point in *Xenopus* meiotic maturation. Nature 374:511–516.

Smith LD (1989): The induction of oocyte maturation: Transmembrane signaling events and regulation of the cell cycle. Development 107:685–699.

Smit-McBride Z, Privalsky ML (1993): Functional domains of the v-*erbA* protein necessary for oncogenesis are required for transcriptional activation in *Saccharomyces cerevisiae*. Oncogene 8:1465–1475.

Steinert G, Baltus E, Hanocq-Quertier J, Brachet J (1974): Ultrastructure of *Xenopus laevis* oocytes after injection of an extract from progesterone-treated oocytes. J Ultrastruct Res 49:188–210.

Subauste JS, Koenig RJ (1995): Comparison of the DNA binding specificity and function of v-ErbA and thyroid hormone receptor α1. J Biol Chem 270:7957–7962.

Thompson CC, Evans RM (1989): Trans-activation by thyroid hormone receptors: Functional parallels with steroid hormone receptors. Proc Natl Acad Sci U S A 86:3494–3498.

Török I, Strand D, Schmitt R, Tick G, Török T, Kiss I, Mechler BM (1995): The *overgrown hematopoietic organs-31* tumor suppressor gene of *Drosophila* encodes an *importin*-like protein accumulating in the nucleus at the onset of mitosis. J Cell Biol 129:1473–1489.

Wasserman WJ, Masui Y (1975): Effects of cycloheximide on a cytoplasmic factor initiating meiotic maturation in *Xenopus* oocytes. Exp Cell Res 91:381–388.

Yew N, Mellini ML, Vande Woude GF (1992): Meiotic initiation by the *mos* protein in *Xenopus*. Nature 355:649–652.

Zhang X-K, Wills KN, Husmann M, Hermann T, Pfahl M (1991): Novel pathway for thyroid hormone receptor action through interaction with *jun* and *fos* oncogene activities. Mol Cell Biol 11:6016–6025.